Available online at www.sciencedirect.com
ScienceDirect
Polymer 48 (2007) 6086–6096
polymer
www.elsevier.com/locate/polymer

Effects of aspect ratio of MWNT on the flammability properties of polymer nanocomposites ☆

Bani H. Cipiriano [a], Takashi Kashiwagi [b,*], Srinivasa R. Raghavan [a], Ying Yang [c], Eric A. Grulke [c], Kazuya Yamamoto [b], John R. Shields [b], Jack F. Douglas [d]

[a] Department of Chemical and Biomolecular Engineering, University of Maryland, College Park, MD 20742, USA
[b] Fire Research Division, National Institute of Standards and Technology, Gaithersburg, MD 20899, USA
[c] Department of Chemical and Materials Engineering, University of Kentucky, Lexington, KY 40506, USA
[d] Polymers Division, National Institute of Standards and Technology, Gaithersburg, MD 20899, USA

Received 6 July 2007; received in revised form 30 July 2007; accepted 31 July 2007
Available online 6 August 2007

Abstract

The effects of the aspect ratio of multi-walled carbon nanotubes (MWNTs) on the rheology and flammability of polystyrene/MWNT nanocomposites are studied using two MWNTs having average aspect ratios (length to outer diameter) of 49 and 150. Dynamic rheological experiments show that the particles with the larger aspect ratio impart much higher storage moduli and complex viscosities to the nanocomposites compared to equivalent mass loadings of particles with the smaller aspect ratio. Additionally, in flammability experiments, the larger aspect ratio particles lead to a greater reduction in mass loss rate, i.e., they are more effective at reducing flammability. These results demonstrate that the aspect ratio of MWNTs is a key parameter in controlling the rheology and flammability of polymer nanocomposites.
Published by Elsevier Ltd.

Keywords: Aspect ratio; Flammability; Nanocomposites

1. Introduction

Polymer nanocomposites have attracted a great deal of interest due to their ability to improve physical properties of polymers such as mechanical and thermal properties. In particular, polymer–carbon nanotube nanocomposites have been extensively studied to explore their unique electronic, thermal, optical, and mechanical properties [1–5], as summarized in recent review articles [6,7]. Furthermore, an improvement in the flammability properties of polymers has been achieved with polymer–carbon nanotube nanocomposites, which could provide an alternative to conventional flame retardants [8–15]. The outstanding improvement of physical properties with carbon nanotubes is in part attributed to their extremely high aspect ratio (length to outer diameter ratio) of up to 1000. An increase in the aspect ratio of single-walled carbon nanotube (SWNT) increases Young's modulus [16] and reduces critical concentration for the formation of a percolation network [17]. Other evidence includes higher electric and thermal conductivities of epoxy–carbon nanotube nanocomposites with high aspect ratio of the tubes [18] and higher thermal conductivity of poly α-olefin/multi-walled carbon nanotube nanocomposites [19]. Furthermore, polymer–clay nanocomposites with higher aspect ratios (length to thickness ratio) of clay particles are also found to have enhanced barrier [20,21] and mechanical properties [22–24].

Although many studies have shown enhanced physical properties of polymer nanocomposites with increasing aspect ratio, only a limited study on the effects of aspect ratio of nanoparticles on flammability properties of polymer

☆ This was carried out by the National Institute of Standards and Technology (NIST), an agency of the US Government which, by statute, is not subject to copyright in US.

* Corresponding author.
E-mail address: takashi.kashiwagi@nist.gov (T. Kashiwagi).

0032-3861/$ - see front matter Published by Elsevier Ltd.
doi:10.1016/j.polymer.2007.07.070

nanocomposites has been reported. In particular, the measurement has been limited to clay nanocomposites [25]. The objective of this study is to determine the effects of aspect ratio of MWNT on the flammability properties of polystyrene. It has been demonstrated that the formation of a jammed network composed of carbon nanotubes in the initial composite samples is critical to significantly reduce the heat release rate of the composites [15]. Therefore, dynamic measurement of storage modulus of the samples is made at an elevated temperature to determine the effects of aspect ratio of MWNT on network formation in these materials.

2. Experimental

2.1. Materials

The matrix polymer used in this study was PS (Styron 666D, Dow Chemical, melt mass flow rate of 8.0 g/10 min at 200 °C).[1] Two different MWNTs were used; one was purchased from Hyperion Catalyst International in the form of a master batch with a mass concentration of 20% in PS. Other MWNTs were made using xylene as a carbon source and ferrocene as a catalyst at about 675 °C by a chemical vapor deposition, CVD, method at the University of Kentucky [26].

2.2. Composites

Composites were prepared at the University of Kentucky by melt blending the MWNT–polystyrene mixture in a Haake PolyLab shear mixer. The mixture temperature was set at 180 °C and the polystyrene pellets were added to the mixer running at a speed of 20 rpm. The pellets melted in about 3 min, and the MWNTs were added at this time and mixing was continued for 40 min. For the Hyperion master batch, appropriate amounts of the PS pellets and of the master batch pellets were mixed and fed into a B & P Process Equipment and Systems twin-screw extruder (co-rotating, intermeshing, *L*:*D* equals 25:1) at NIST. Operating conditions were 400 rpm screw speed and 185 °C barrel temperature in all zones except the last zone (195 °C). Samples with mass concentrations of 0.2%, 0.5%, 1%, 2%, and 4% MWNT were prepared with the two MWNTs. All samples for measuring flammability properties (discs of 75 mm diameter and 4 mm thickness) were compression molded at 200 °C under a pressure of about 1.4 MPa for a duration of 15 min.

2.3. Sample characterization

The morphologies of the nanotubes in the melt blended samples were evaluated using a laser confocal microscope (Model LSM510, Carl Zeiss Inc.) to image the MWNTs in the PS matrix. The confocal microscope utilizes coherent laser light and collects reflected light exclusively from a single plane with a thickness of 100 nm (a pinhole sits conjugated to the focal plane and rejects light out of the focal plane). A red laser ($\lambda = 633$ nm) was used as the coherent light and images were taken at 100× magnification with an Epiplan-Neofluar 100×/1.30 oil-pool objective. An LP385 (Rapp Opto Electronic) filter was used to limit the lower spectra of reflected light. One hundred two-dimensional images (optical slices with 512 pixels × 512 pixels), with scan size 92.1 × 92.1 μm, were taken at a spacing of 100 nm by moving the focal plane.

The aspect ratio of the MWNTs was evaluated using scanning and transmission electron microscopies (SEM and TEM). The SEM, Phillips ESEM – E3, was operated at a voltage of 30 kV. The TEM, Hitachi H-600, was operated at a voltage of 100 kV. MWNTs were isolated from the nanocomposite by extraction of polystyrene in tetrahydrofuran, THF. The MWNTs were then dried and redispersed at very low concentrations (~0.01 mg/mL) in THF by stirring. Ultrasonication was avoided since it is known to modify nanotube length. Drops of the MWNT dispersion in THF were dried onto the freshly cleaved mica surfaces for evaluation using SEM. Nitrogen was blown on the drops to vaporize the THF quickly and prevent substantial tube aggregation. For evaluation using TEM, drops of the dispersion were dried onto a copper grid covered with carbon film (Ted Pella, Redding, CA).

Rheological experiments were performed on an RDAIII strain-controlled rheometer (TA Instruments) equipped with a convection oven. A parallel plate geometry (25 mm diameter) was used with a gap of 0.9 mm. Samples were prepared by melt-pressing nanocomposite pellets at 150 °C and a pressure of about 0.93 MPa. All rheological experiments were performed at 200 °C and in a nitrogen atmosphere to avoid oxidative degradation of polystyrene. The gap reference was set at 200 °C. Dynamic rheological experiments were conducted to measure the storage and loss moduli as a function of frequency (0.01–100 rad/s) at a constant strain of 0.5% (this value of strain was verified to be in the linear viscoelastic regime of the sample). Thermogravimetric analysis (TGA) was conducted using a TA Instruments TGA Q500 at a heating rate of 5 °C/min from 90 °C to 500 °C in nitrogen (flow rate of 60 cm^3/min) for the original nanocomposite samples (about 5 mg) in a platinum pan.

2.4. Flammability property measurement

A cone calorimeter built by NIST was used to measure ignition characteristics, heat release rate, and sample mass loss rate according to ASME E1354/ISO 5660. An external radiant heat flux of 50 kW/m^2 was applied. All of the samples were measured in the horizontal position and wrapped with a thin aluminum foil except for the irradiated sample surface. The standard uncertainty of the measured heat release rate was ±10%.

A radiant gasification apparatus, somewhat similar to a cone calorimeter, was designed and constructed at NIST to study the gasification processes of samples by measuring

[1] Certain commercial equipment, instruments, materials, services or companies are identified in this paper in order to specify adequately the experimental procedure. This in no way implies endorsement or recommendation by NIST.

mass loss rate and temperatures of the sample exposed to a fire-like heat flux in a nitrogen atmosphere (no burning). The apparatus consists of a stainless-steel cylindrical chamber that is 1.70 m tall and 0.61 m in diameter. In order to maintain a negligible background heat flux, the interior walls of the chamber are painted black and the chamber walls are water-cooled to 25 °C. All experiments were conducted at 50 kW/m^2. The unique nature of this device is threefold: (1) observation and results obtained from it are only based on the condensed phase processes due to the absence of any gas phase oxidation reactions and processes; (2) it enables visual observations of gasification behavior of a sample using a video camera under a radiant flux similar to that of a fire without any interference from a flame; (3) the external flux to the sample surface is well-defined and nearly constant over the duration of an entire experiment (and over the spatial extent of the sample surface) due to the absence of heat feedback from a flame. A more detailed discussion of the apparatus is given in a previous study [27]; the standard relative uncertainty of the measured mass loss rate is ±10%.

3. Results

3.1. Aspect ratio and morphology of the MWNTs in PS

TEM images of the two types of MWNTs studied here (from Kentucky and Hyperion, respectively) are shown in Fig. 1. In order to determine the aspect ratio for both types of MWNTs, it is important to extract the MWNTs from compounded PS/MWNT samples because particle sizes might be modified during extrusion. A minimum of 140 measurements of diameter and of 200 measurements of length was conducted for both types of MWNTs. Histograms of MWNT length and diameter are shown in Fig. 2 for the extracted Kentucky MWNTs and in Fig. 3 for the Hyperion MWNTs. The average diameter and length of the Kentucky MWNTs were obtained by SEM (images not shown) and they are 75 ± 54 nm and 11.3 ± 5.6 μm, respectively. The dimensions of the Hyperion MWNTs were determined by using TEM and they are 7.1 ± 2.5 nm and 351 ± 195 nm, respectively. The large standard deviation was mainly due to a few large or extremely long and large tubes, as shown in Figs. 2 and 3. The average aspect ratio obtained by dividing the average length by the average diameter is 150 for the Kentucky MWNTs and 49 for the Hyperion MWNTs. Henceforth, the Kentucky MWNTs will be designated as MWNT-150 and the Hyperion MWNTs as MWNT-49.

Since a good dispersion of the nanotubes in the polymer matrix is crucial for the reduction in flammability [14,28], the distribution of the tubes in the PS/MWNT samples was examined by confocal microscopy to globally observe the dispersion of the MWNTs, as shown in Fig. 4. Each MWNT-150 tube can be seen in the figure and these tubes are well dispersed in PS without forming many agglomerates. However, the confocal microscopy has barely enough spatial resolution to see each MWNT-49 tube due to its much smaller size than MWNT-150. All images show no formation of agglomerates except some possibility in the image of Fig. 4(b). From these images and others (not shown), we consider that both tubes were reasonably well dispersed in PS.

3.2. Thermal stability

Thermogravimetric analysis was conducted in nitrogen at a heating rate of 5 °C/min. Although previous studies did not conclusively exclude the effects of oxygen in surrounding air on thermal degradation of polymeric materials during burning of polymers, oxidation reactions of the polymers appear to be insignificant (oxygen is mainly consumed by gas phase reactions, i.e., the flame). An exception is the case in which the flame does not cover the entire burning surface or the burning/pyrolysis rate is extremely low [29,30]. Addition of either MWNT-150 or MWNT-49 to PS does not show significant effects on thermal stability of PS even with significant mass concentration of MWNTs, as shown in Fig. 5.

3.3. Viscoelastic properties

We previously found that nanocomposites based on carbon nanotubes are capable of forming a continuous network-structured protective layer that mainly consists of the tubes without the formation of any opening/cracks [14,15]. (Vigorous

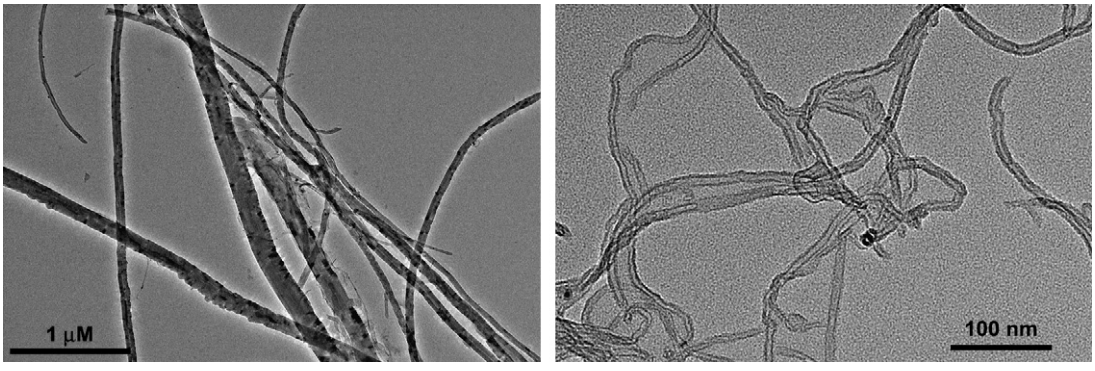

Fig. 1. TEM images of the MWNTs extracted from the composites, left is MWNTs in PS/MWNT prepared at University of Kentucky and right is MWNTs in PS/MWNT compounded with the Hyperion master batch.

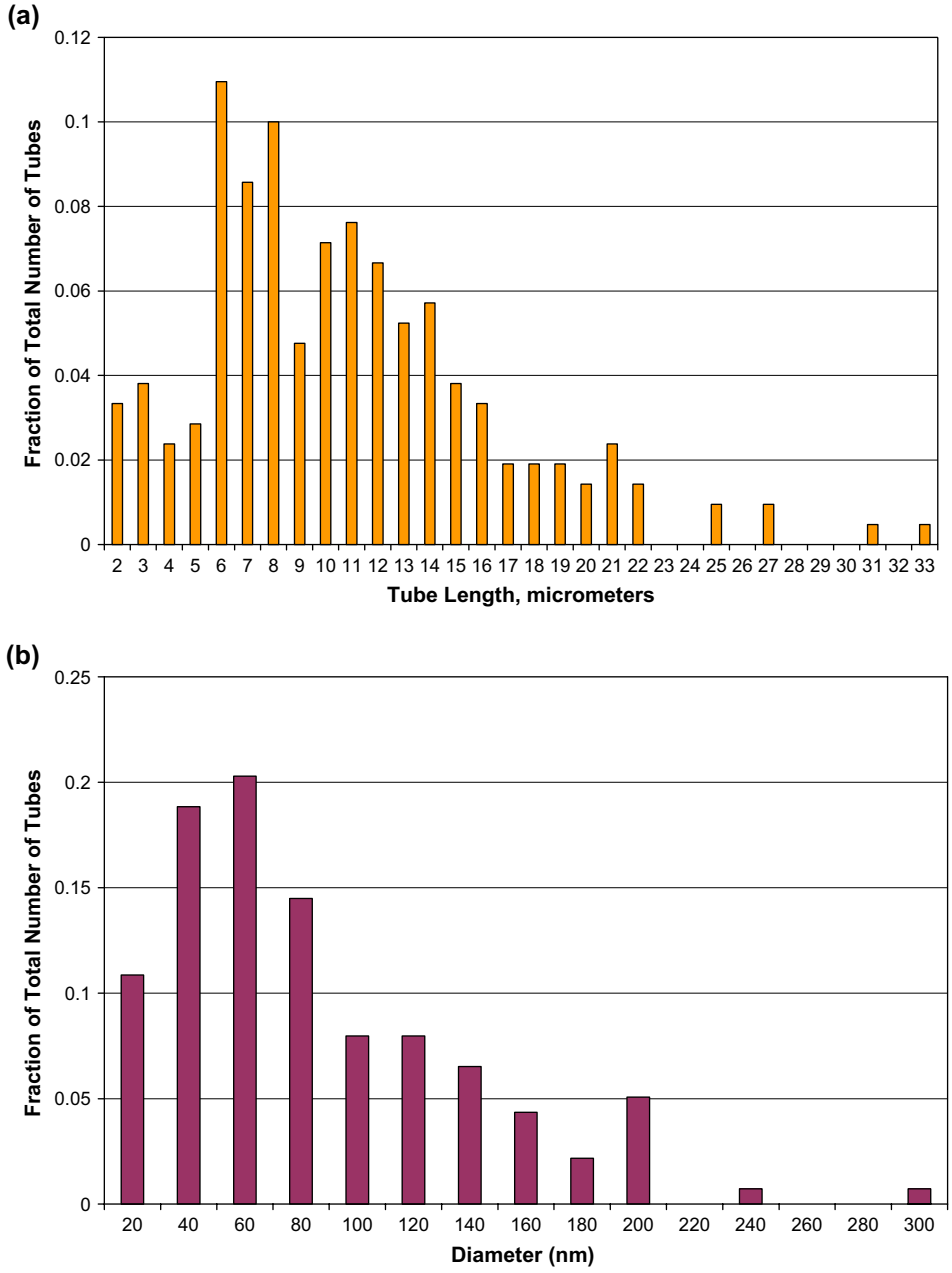

Fig. 2. Histogram plots of the dimension of MWNT, prepared at the University of Kentucky, extracted from the compounded PS/MWNT: (a) tube length and (b) tube diameter.

bubbling through any opening/cracks supplies evolved combustible degradation products to a flame, which compromises the flame retardant effectiveness.) This results in a significant reduction in heat release rate (a flammability measure related to the intensity/size of fire; the lower the heat release rate, the smaller the size of fire) with a carbon nanotube mass concentration as low as 0.5% [15]. Since the network is formed in the initial composite samples, flame retardant effectiveness could be estimated from the measurement of storage modulus of the initial samples. The storage modulus G' provides a measure of nanocomposites' 'stiffness' and its frequency dependence characterizes whether the material is liquid-like or solid-like.

Fig. 6 plots G' for PS/MWNT composites made from the MWNTs of two different aspect ratios. At 200 °C, the G' curve of PS shows the typical response of a viscous liquid with $G' \sim \omega^2$ at low frequencies ω. At a 1% MWNT loading, the G' of PS/MWNT-49 is slightly higher than that of PS, while the G' of PS/MWNT-150 is even higher. At higher mass concentrations of MWNTs, the liquid-like low-frequency scaling of G' disappears and G' becomes nearly constant at low frequencies. We term the composition at which this rheological state is achieved as the 'gel concentration', φ_g. We define φ_g as the concentration at which G' becomes independent of φ for an extended low-frequency range. The φ_g of the composites with MWNT-150 is between 1% and 2% compared to about 4% with MWNT-49.

Fig. 7 plots the storage modulus measured at a frequency of 0.5 rad/s for PS/MWNT-150 and PS/MWNT-49 as a function

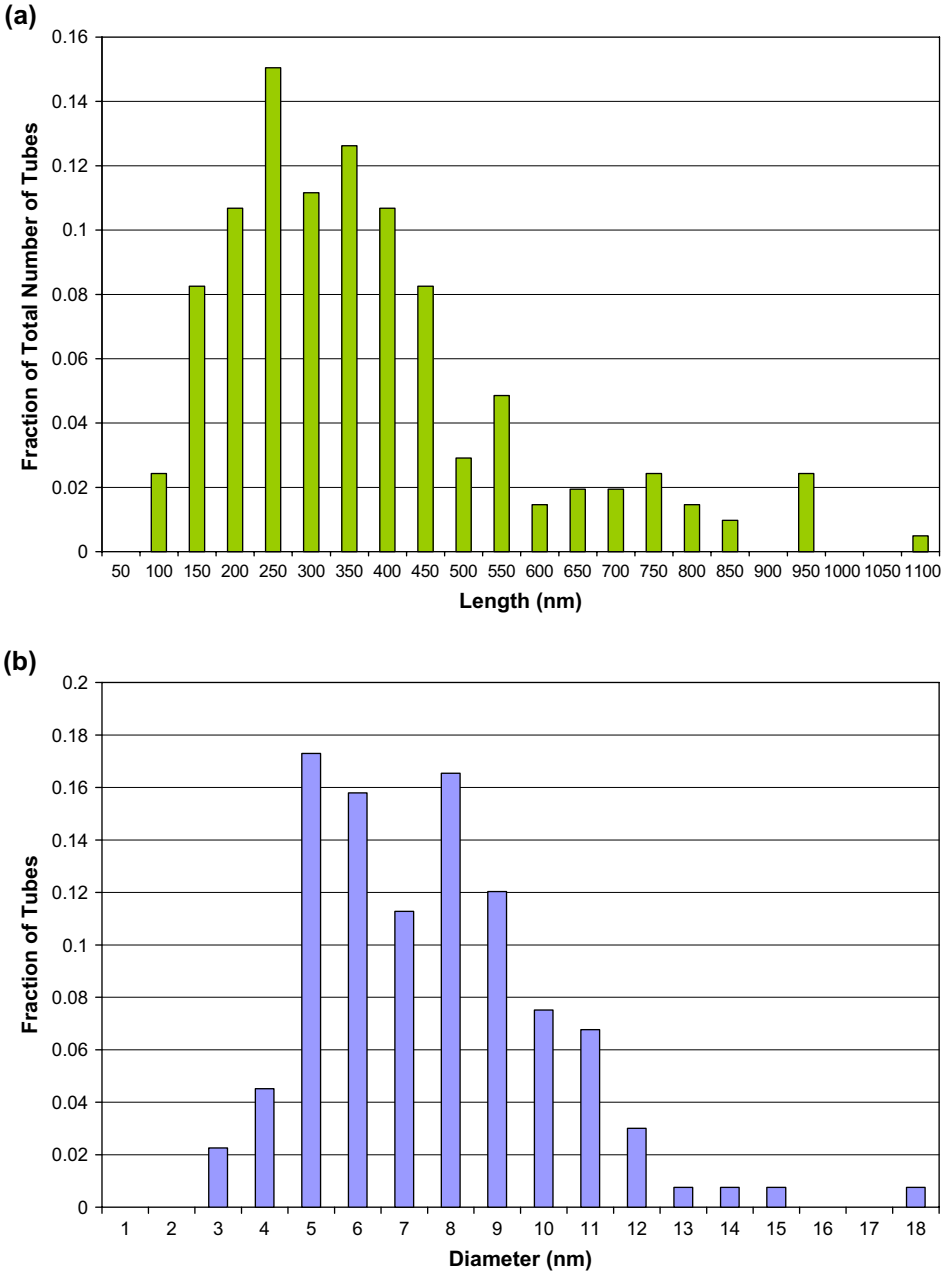

Fig. 3. Histogram plots of the dimension of MWNT in PS/MWNT compounded with the Hyperion master batch: (a) tube length and (b) tube diameter.

of MWNT concentration. This data reiterate that the G' for MWNT-150 composites is significantly larger than that for MWNT-49 at all mass concentrations studied. Note that at a mass concentration of 0.1% with MWNT-150 and 0.1% and 0.2% with MWNT-49 the G' of the composites are less than that of pristine PS. This reduction in G' is due to a small reduction in molecular weight of PS during compounding, and similar reduction in G' has been observed for extruded polymer–clay composites at low clay concentrations [31,32]. If we define a percolation concentration of MWNT, φ_c, as the concentration when the intertube interactions dominate over polymer chain interactions, φ_c for PS/MWNT-150 is about 0.35% and that for PS/MWNT-49 is 0.62%. It has been known that a bulk 'stiffness' G' of the composites varies phenomenologically with mass concentration according to a power law [17,33]

$$G'/G'_{PS} \sim [(\varphi - \varphi_c)/\varphi_c]^{\beta}$$

The inset in Fig. 7 shows that the above relationship adequately describes the G' data for both PS/MWNT-150 and PS/MWNT-49, with the value of $\beta = 2$ for the former and 2.3 for the latter. Indeed, $\beta = 2$ is a typical experimental value for networks of stiff fibers [35].

We now consider the effects of aspect ratio and mass concentration of MWNT on complex viscosity at 200 °C (Fig. 8).

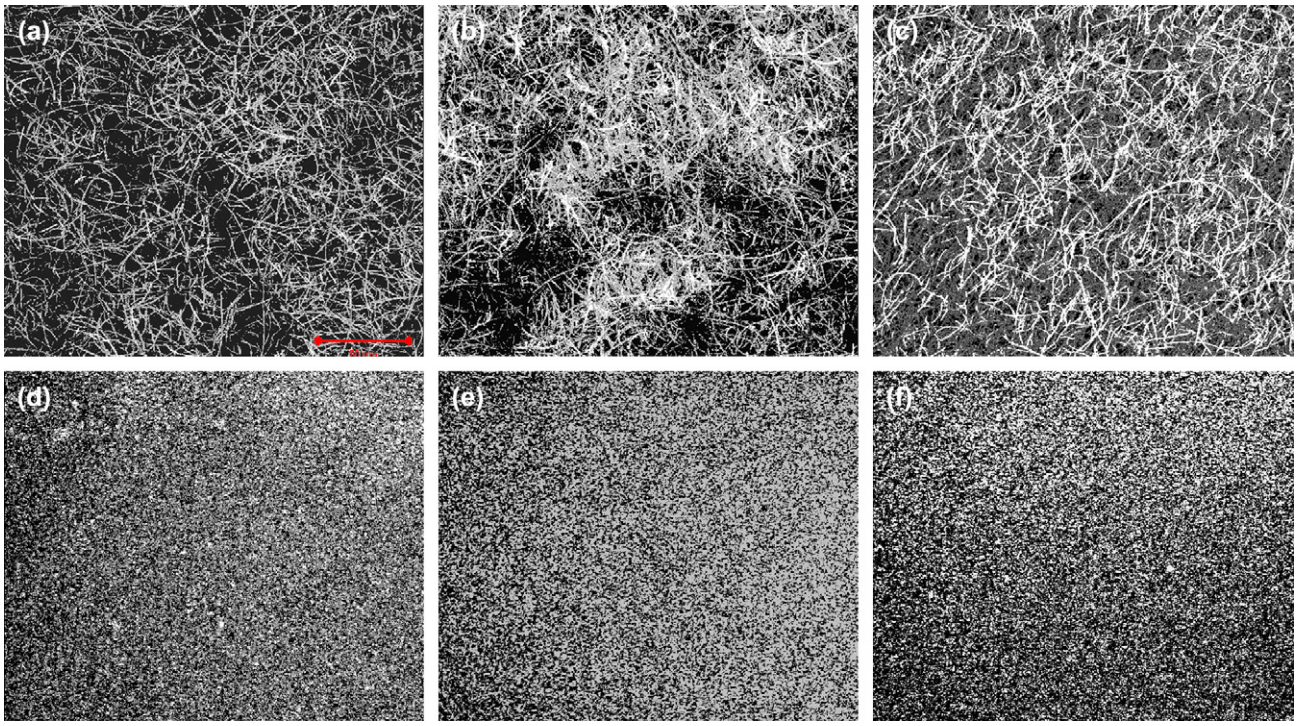

Fig. 4. Confocal microscopic images with a scale bar of 20 μm : (a) PS/MWNT-150 (1%), (b) PS/MWNT-150 (2%), (c) PS/MWNT-150 (4%), (d) PS/MWNT-49 (1%), (e) PS/MWNT-49 (2%), and (f) PS/MWNT-49 (4%).

Since suppression of bubbling caused by the nucleation of degradation products in the polymer melt [34] is required for effective flame retardant performance, the melt viscosity of the composites at elevated temperatures might play an important role in this process. The data in Fig. 8 show an increase by about two orders of magnitude in the complex viscosity at low frequencies upon addition of 4% MWNTs. This significant increase in complex viscosity indicates an increasing importance of tube–tube interactions in dictating the rheological response [35,36]. Fig. 8 also shows that the complex viscosities of the composites with MWNT-150 are higher than those with MWNT-49 at the same mass concentration (similar to the trend in Figs. 6 and 7 for G'). These results suggest that the PS/MWNT-150 samples should be less flammable than those of PS/MWNT-49 at the same MWNT concentration.

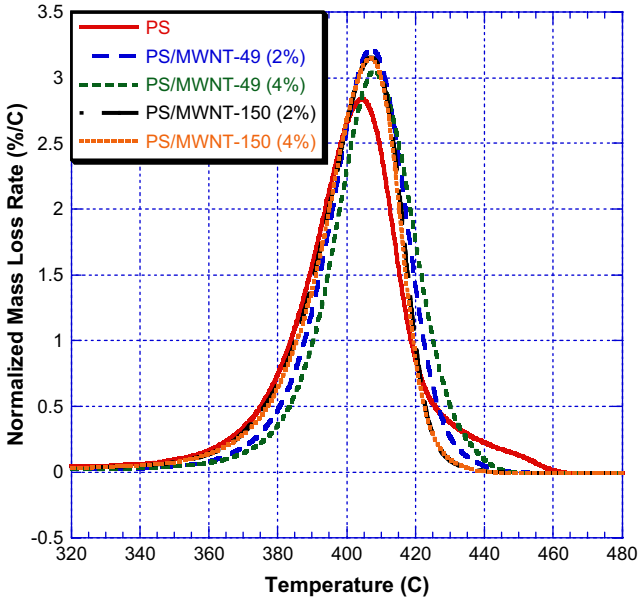

Fig. 5. Derivative thermogravimetric mass loss rates of selected samples.

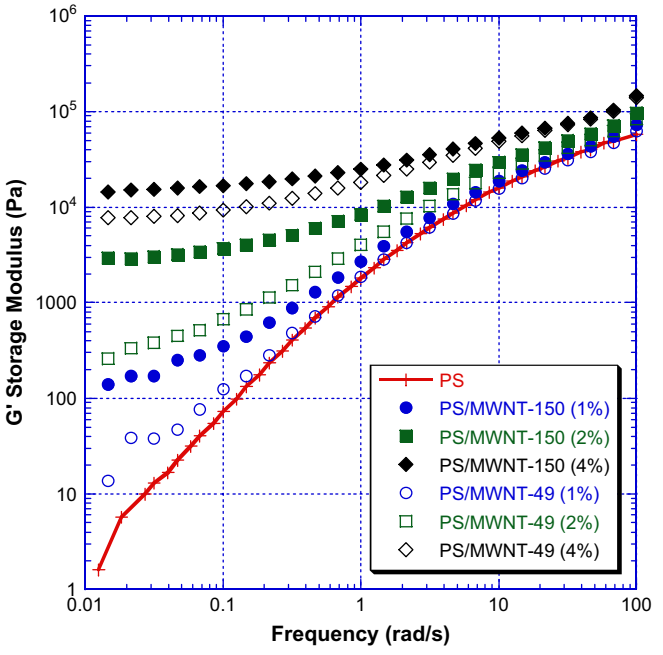

Fig. 6. Effects of aspect ratio and of mass concentration of MWNT on storage modulus of PS/MWNT nanocomposites at 200 °C.

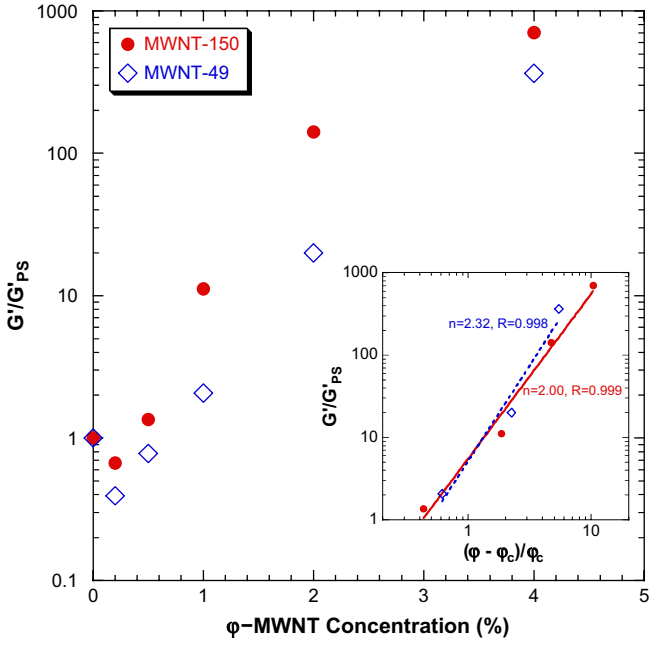

Fig. 7. The relationship between mass concentration of MWNT and normalized storage modulus of PS/MWNT nanocomposites at a frequency of 0.05 rad/s and 200 °C with that of PS. Inset is the power law relationship between the normalized storage modulus and normalized mass concentration of MWNT with percolation mass concentration P_c.

3.4. Flammability properties

The mass of a sample was continuously measured under an external radiant flux of 50 kW/m^2 in a slow flowing nitrogen atmosphere and mass loss rate was calculated by taking the time derivative of the measured weight change. The results with PS/MWNT-150 and with PS/MWNT-49 at various mass concentrations of the MWNT are shown in Fig. 9(a) and (b), respectively. At low mass concentrations of both MWNTs, the reduction in mass loss rate was relatively small. The nanocomposites behaved like a liquid with numerous bubbles

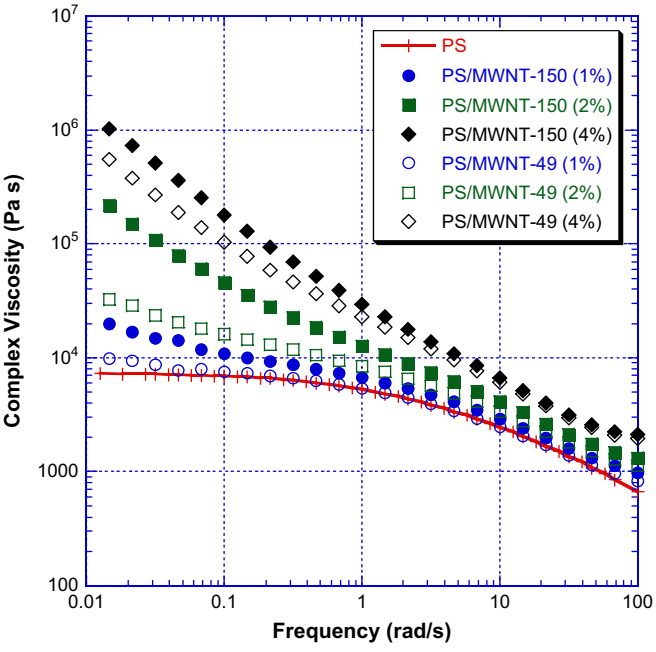

Fig. 8. Effects of aspect ratio and of mass concentration of MWNT on complex viscosity of PS/MWNT nanocomposites at 200 °C.

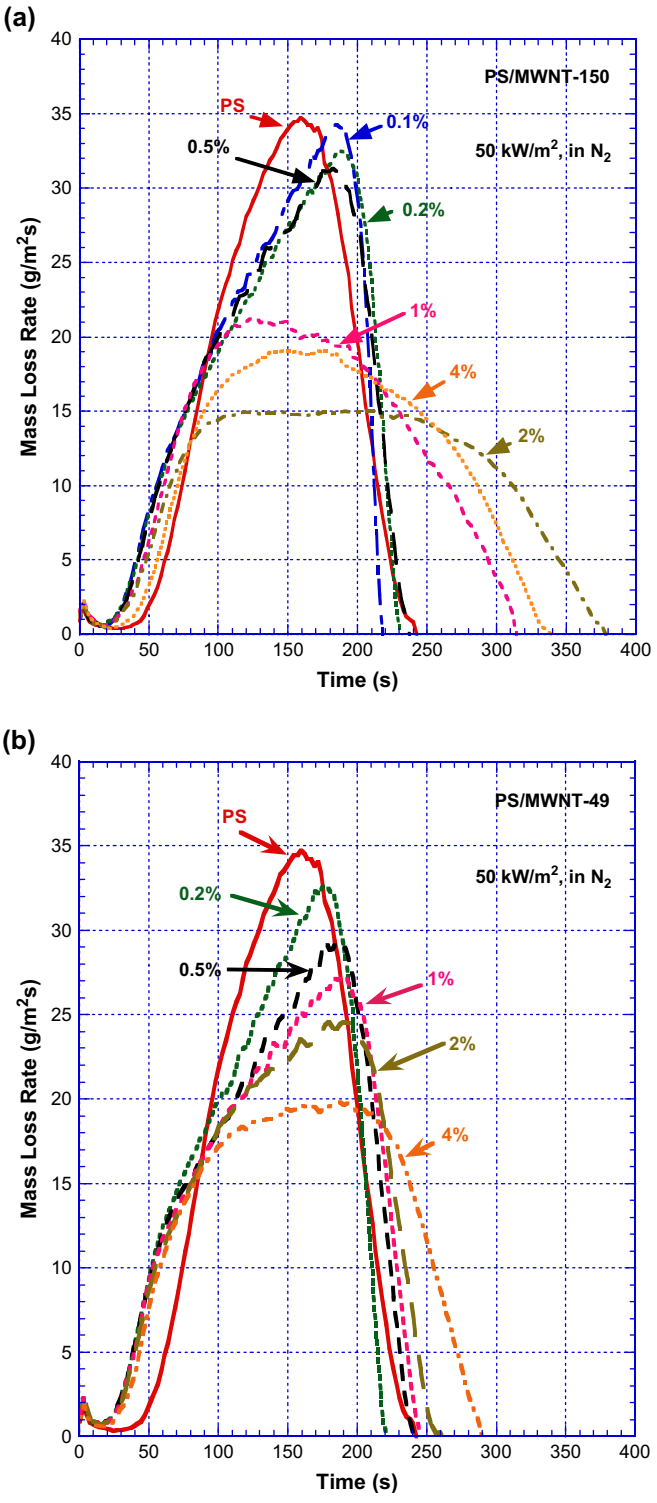

Fig. 9. Effects of mass concentration of MWNT on mass loss rate of PS/MWNT nanocomposites at 50 kW/m^2 in *nitrogen*: (a) samples with MWNT-150 and (b) with MWNT-49.

during the test and no char was left in the container. Also, samples with low mass concentrations of either of the MWNTs behaved like a viscous liquid with accompanying formation and bursting of many large bubbles and formation of many small black islands. Such islands were left at the end of the test as can be seen in the images shown in Fig. 10. The number and size of the islands increased with an increase in mass concentration of MWNTs. With 1% of MWNT-150, the sample behaved almost like a solid with a wavy surface contour; PS/MWNT-150 (2%) and PS/MWNT-150 (4%) also behaved like a solid forming a uniform protective layer with a smooth surface without any openings. This protective layer has a randomly interlaced network structure mainly consisting of the MWNTs [10,14]. PS/MWNT-150 (2%) has the lowest mass loss rate as shown in Fig. 11. However, PS/MWNT-150 (4%) has higher peak mass loss rate than that of PS/MWNT-150 (2%). The measured transmitted heat flux through the residue of PS/MWNT-150 (4%) collected after the gasification test was about 15 kW/m^2 compared to about 12.5 kW/m^2 for the residue of PS/MWNT (2%). This higher transmitted heat flux for the residue of PS/MWNT-150 (4%) is due to an increase in thermal conductivity of the sample at high MWNT mass concentration [10]. The sample with higher thermal conductivity tends to slow the increase in initial mass loss rate but to increase it later after accumulation of energy in the sample. The mass loss rate of PS/MWNT-49 decreases with an increase in mass concentration of the tubes, but the peak mass loss rate tends to be higher than that of PS/MWNT-150 at the same mass concentration of tubes. It appears that true percolation-like behavior is not responsible for the reduction in mass loss rate of PS/MWNT-49. The residue even at 4% mass concentration consisted of numerous granular, coarse particles, as shown in Fig. 10, instead of a uniform protective layer. Bubbling in the space between the particles could be seen during the test.

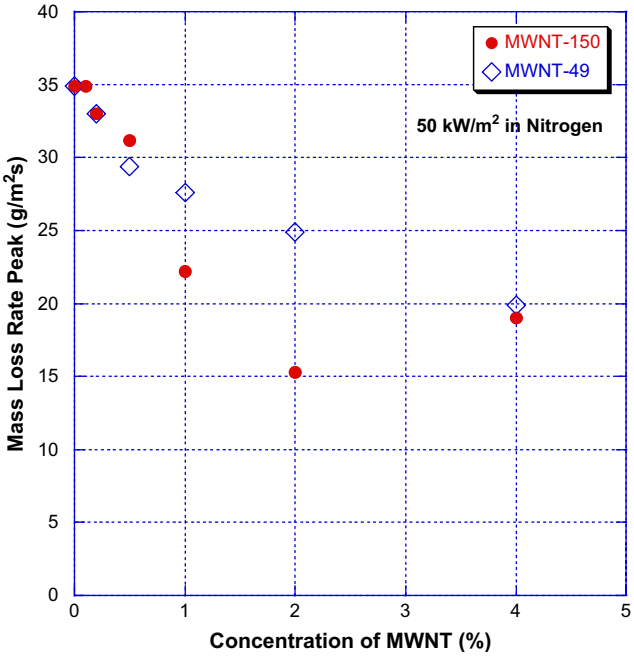

Fig. 11. The effects of aspect ratio of MWNT on the relationship between mass loss rate peak and mass concentration of MWNT.

It has been demonstrated that the flame retardant performance of polymer–carbon nanotube nanocomposites is mainly due to the physical process of heat shielding by the formation of a network-structured protective layer in the condensed phase [10,14,15]. Therefore, it is expected that the heat release rate curves of these samples would be similar to the mass loss rate curves shown in Fig. 9. Observed heat

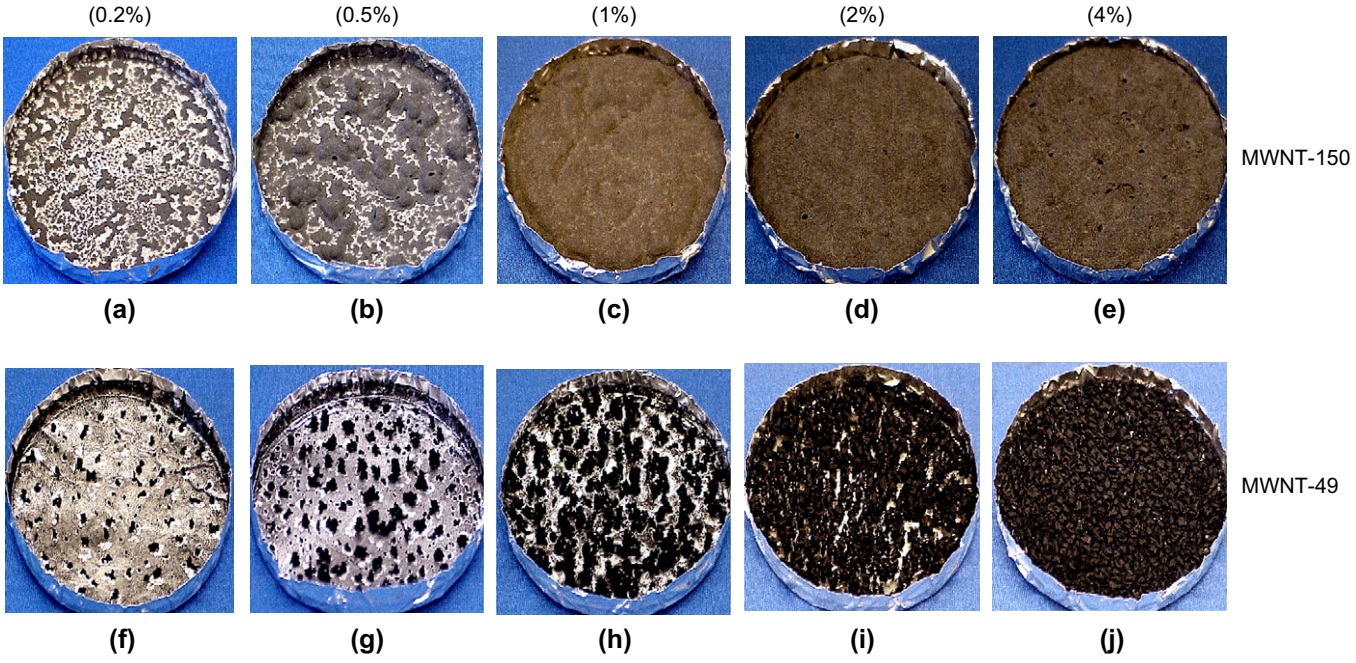

Fig. 10. Comparison of residues of PS/MWNT nanocomposites, based on MWNT-150 and MWNT-49, collected after the gasification test at 50 kW/m^2 in nitrogen.

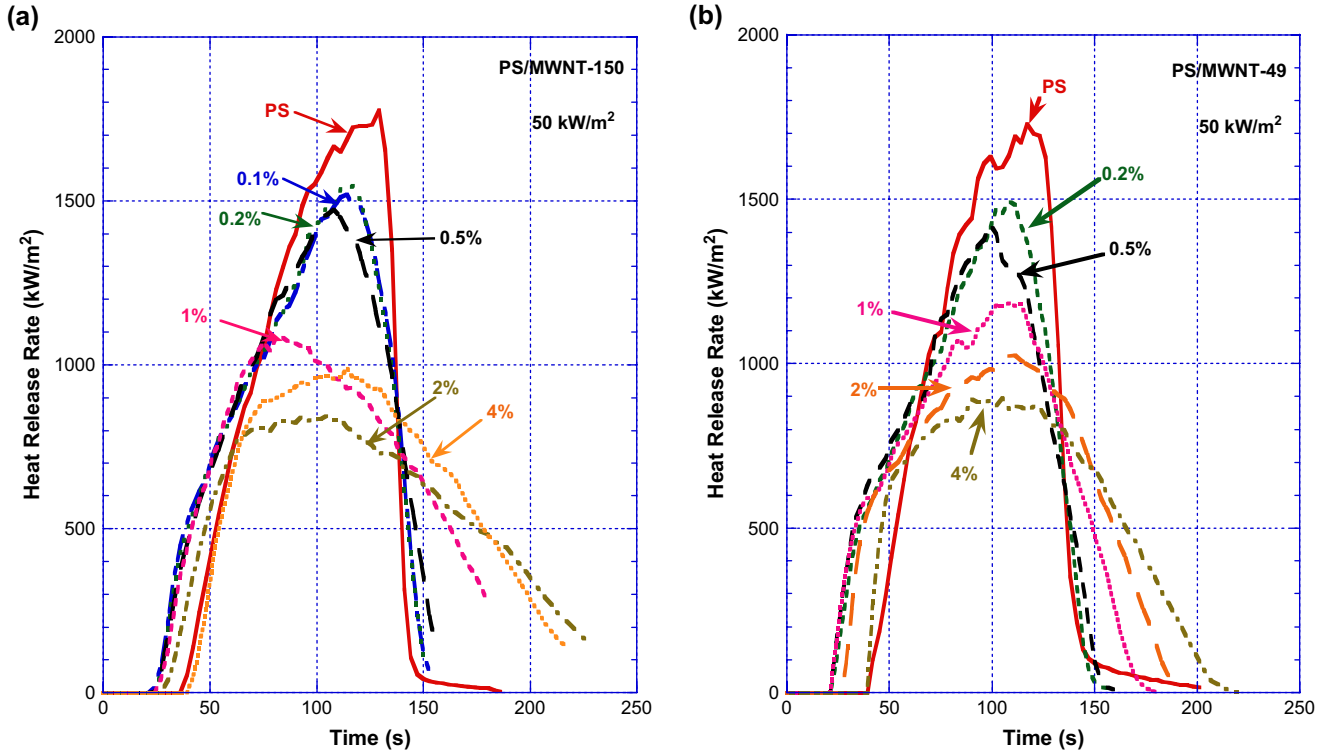

Fig. 12. Heat release rate curves of PS/MWNT nanocomposites at various mass concentrations of MWNT at 50 kW/m^2: (a) with MWNT-150 and (b) with MWNT-49.

release rate curves with the two different MWNTs at various mass concentrations of the tubes are shown in Fig. 12. The observed trends are very similar to those observed in Fig. 9, including lower peak heat release rates for PS/MWNT-150 as compared to those of PS/MWNT-49 at the same tube mass concentration. Furthermore, the peak heat release rate of PS/MWNT-150 (4%) is higher than that of PS/MWNT-150 (2%) as observed in Fig. 9 due to an increase in thermal conductivity for PS/MWNT-150 (4%) as described above.

4. Discussion

The above results clearly show the importance of aspect ratio of MWNT on viscoelastic properties and flammability properties of PS/MWNT nanocomposites. Since the sizes of the two MWNTs are quite different, it is interesting to explore the significant effects of the aspect ratio. We estimate the difference in the total number of MWNTs in PS/MWNT-150 (average length of 11 μm and average outer diameter of 97 nm) and PS/MWNT-49 (average length of 347 nm and average diameter of 7.1 nm) at the same mass concentration of MWNT. With the assumptions that the outer diameter is much larger than the inner diameter of both tubes and that both the densities of the two MWNTs are the same, the total number of MWNT-49 is roughly 6000 times more than that of MWNT-150 in the same volume of PS/MWNT. Furthermore, the total outer surface area of MWNT-49 in PS/MWNT-49 is about 14 times greater than that of MWNT-150 in PS/MWNT-150. However, the results show that the effects of aspect ratio of MWNT are more dominant than the total number of nanotubes or their total surface area. Then, if two MWNT types having the same outer diameter but different aspect ratios (different lengths of tube) were used, it is possible that the effects of aspect ratio on flammability properties might be larger than those observed in this study.

The importance of aspect ratio of nanoparticles on the formation of the network-structured layer and flammability properties was also demonstrated in our previous study with plate shaped nanoparticles of clay [25]. In that study three different types of clays were used in polypropylene/polypropylene-*g*-maleic anhydrate (PP/PP-*g*-MA): synthetic mica (aspect ratio of about 1200 [37]), montmorillonite (MMT) (about 200 [37]) and synthetic hectorite (about 50 [37]). The sample was a 10 cm × 10 cm × 0.3 cm thick plate and it was tested in nitrogen at 50 kW/m^2. The lowest mass loss rate was observed for the sample with synthetic mica, which generated a significantly lower mass loss rate than with MMT and synthetic hectorite, as shown in Fig. 13. The figure shows pictures of the residues of the four samples collected after the tests. The surface of the residue of the sample with synthetic mica is relatively smooth without any large cracks. However, the two samples with the other two clays show large cracks (in particular, with synthetic hectorite). Melting and vigorous bubbling were observed in the cracks during the test. It has demonstrated that the addition of carbon nanotubes or clay having a large aspect ratio into polymers tends to generate residues having a smooth surface without any openings/cracks and to reduce significantly the flammability properties of the polymers.

In Fig. 6, the storage modulus of PS/MWNT-49 (4%) is seen to be nearly independent of frequency at low frequencies,

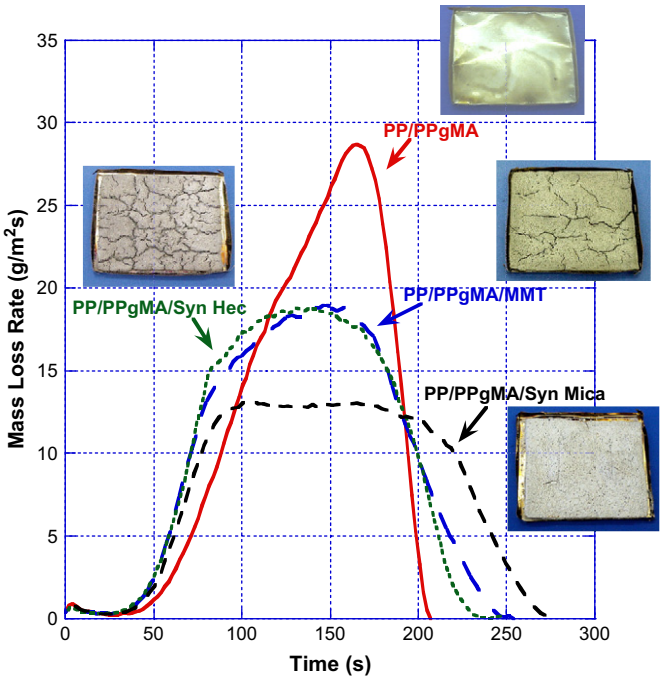

Fig. 13. Effects of clay type on mass loss rate of PP (92.3%)/PP-*g*-MA (7.7%) and PP (84.6%)/PP-*g*-MA (7.7%)/clay (7.7%) samples in nitrogen at 50 kW/m^2.

which indicates the formation of network structure and such nanocomposite samples having a relatively high complex viscosity formed a protective heat shield layer covering the sample surface without any cracks [10,12,15]. However, it appears that the residue of PS/MWNT-49 (4%) collected after the gasification test in nitrogen at 50 kW/m^2 is made of a collection of numerous discrete agglomerates, as shown in Fig. 10j. Vigorous bubbling was observed around the agglomerates during the test and the mass loss rate of this sample is not as low as that of PS/MWNT-150 (2%) which did form a smooth, network-structured protective layer, as shown in Fig. 10d. In our previous study, the formation of the network-structured protective layer was observed with poly(methyl methacrylate)/single-walled carbon nanotube (PMMA/SWNT) nanocomposite at a mass concentration of 0.5% [15]. The aspect ratio of the bundled SWNT was about 45 based on the average diameter of about 7 nm and average length of 310 nm. Since these SWNT bundles and MWNT-49 are about the same size, the size of MWNT-49 is not the reason why PS/MWNT-49 does not form the protective layer. If the dispersion of MWNT-49 in PS/MWNT-49 (4%) is much worse than that of MWNT-150 in PS/MWNT-150 (this does not appear in Fig. 4), the storage modulus of PS/MWNT-49 (4%) should not be so high as shown in Fig. 6. At present, it is not clear why a fully effective protective layer was not formed for PS/MWNT-49.

5. Conclusions

The effects of the aspect ratio of MWNT on viscoelastic properties and flammability properties of PS/MWNT nanocomposites were studied with two different MWNTs in the mass concentration from 0.1% to 4%. The samples were prepared using twin-screw extruders. The average aspect ratios of the two MWNTs, 49 and 150, were determined by analyzing the images of the tubes extracted from the compounded nanocomposites, which were taken by SEM and TEM. No significant effects of aspect ratio on thermal stability of PS/MWNT nanocomposites were observed. However, storage modulus and complex viscosity of PS/MWNT-150 are larger than those of PS/MWNT-49 at the same mass concentration of MWNT. PS/MWNT-150 samples with 2% and 4% mass concentration of MWNT-150 form solid-like network structures but only PS/MWNT-49 (4%) forms this structure. The mass loss rate of PS is more reduced with PS/MWNT-150 and the lowest mass loss rate is observed with PS/MWNT-150 (2%). Slightly higher mass loss rate of PS/MWNT-150 (4%) is probably due to an increase in thermal conductivity. With increasing concentration of MWNT-150, the residue of PS/MWNT-150 changes from the formation of discrete islands to a smooth surface layer without any openings, which is generated at concentrations of 2% and 4%. All PS/MWNT-49 samples used in this study did not generate such residues. These results show that the addition of MWNT with large aspect ratios significantly reduces the flammability of polymers.

Acknowledgements

B.H.C. and S.R.R. gratefully acknowledge funding from the NIST BFRL extramural grants program through grant no. 70NANB4H1001. T.K. is funded by NIST under Grant 5D1022.

References

[1] Schadler LS, Giannaris SC, Ajayan PM. Appl Phys Lett 1998;73:3842–4.
[2] Stephan C, Nguyen TP, Lahr B, Blau W, Lefrant S, Chauvet O. J Mater Res 2002;17:396–400.
[3] Dalton AB, Collins S, Munoz E, Razal JM, Ebron VH, Ferraris JP, et al. Nature 2003;423.
[4] Barrau S, Demont P, Peigney A, Laurent C, Lacabanne C. Macromolecules 2003;36:5187–94.
[5] Thostenson ET, Chou T-W. J Phys D Appl Phys 2003;36:573–82.
[6] Coleman JN, Khan U, Blau WJ, Gun'ko YK. Carbon 2006;44:1624–52.
[7] Moniruzzaman M, Winey KI. Macromolecules 2006;39:5194–205.
[8] Kashiwagi T, Grulke E, Hilding J, Harris RH, Awad WH, Douglas JF. Macromol Rapid Commun 2002;23:761–5.
[9] Beyer G. Fire Mater 2002;26:291–3.
[10] Kashiwagi T, Grulke E, Hilding J, Groth K, Harris RH, Butler K, et al. Polymer 2004;45:4227–39.
[11] Peeterbroeck S, Alexandre M, Nagy JB, Pirlot C, Fonseca A, Morea N, et al. Compos Sci Technol 2004;64:2317–23.
[12] Schartel B, Pötschke P, Knoll U, Abdel-Goad M. Eur Polym J 2005;41:1061–70.
[13] Gao F, Beyer G, Yuan Q. Polym Degrad Stab 2005;89:559–64.
[14] Kashiwagi T, Du F, Winey KI, Groth KM, Shields JR, Bellayer SP, et al. Polymer 2005;46:471–81.
[15] Kashiwagi T, Du F, Douglas JF, Winey KI, Harris RH, Shields JR. Nat Mater 2005;4:928–33.
[16] Ashrafi B, Hubert P, Vengallatore S. Nanotechnology 2006;17:4895–903.
[17] Munson-McGee SH. Phys Rev B 1991;43(4):3331–6.
[18] Gojny FH, Wichmann MHG, Fiedler B, Kinloch IA, Bauhofer W, Windle AH, et al. Polymer 2006;47:2036–45.
[19] Yang Y, Grulke EA, Zhang ZG, Wu G. J Appl Phys 2006;99:114307.

[20] Osman MA, Mittal V, Lusti HR. Macromol Rapid Commun 2004;25:1145–9.
[21] Lu C, Mai Y-W. Phys Rev Lett 2005;95:088303.
[22] Miyagawa H, Rich MJ, Drzal LT. J Polym Sci Part B Polym Phys 2004;42:4391–400.
[23] Stretz HA, Paul DR, Li R, Keskkula H, Cassidy PE. Polymer 2005;46:2621–37.
[24] Weon J-I, Sue H-J. Polymer 2005;46:6325–34.
[25] Kashiwagi T. In: Le Bras M, Wilkie CA, Bourbigot S, Duquesne S, Jama C, editors. Fire retardancy of polymers. Cambridge, UK: Royal Society of Chemistry; 2005. p. 81–99 [chapter 6].
[26] Andrews R, Jacques D, Rao AM, Derbyshire F, Qian D, Fan X, et al. Chem Phys Lett 1999;303:467–74.
[27] Austin PJ, Buch RR, Kashiwagi T. Fire Mater 1998;22:221–37.
[28] Kashiwagi T, Fagan J, Douglas JF, Yamamoto K, Heckert AN, Leigh SD. Polymer 2007;48:4855–66.
[29] Brauman SK. J Polym Sci Part B Polym Phys 1988;26:1159–71.
[30] Kashiwagi T, Ohlemiller TJ. Proc Combust Inst 1982;19:815–23.
[31] Wang K, Lian S, Deng J, Yang H, Zhang Q, Fu Q, et al. Polymer 2006;47:7131–44.
[32] Treece MA, Oberhauser JP. Polymer 2007;48:1083–95.
[33] Gingold DB, Lobb CJ. Phys Rev B 1990;42:8220–4.
[34] Kashiwagi T. Proc Combust Inst 1994;25:1423–37.
[35] Kharchenko SB, Douglas J, Obrzut J, Grulke EA, Migler KB. Nat Mater 2004;3:564–8.
[36] Hu G, Zhao C, Zhang S, Yang M, Wang Z. Polymer 2006;47:480–8.
[37] Yano K, Usuki A, Okada A. J Polym Sci Part A Polym Chem 1997;35:2289–94.